

Gold Doesn't Always Glitter: Spectral Removal of Linear and Nonlinear Guarded Attribute Information

Shun Shao Yftah Ziser Shay B. Cohen

Institute for Language, Cognition and Computation

School of Informatics, University of Edinburgh

10 Crichton Street, Edinburgh, EH8 9AB

s.shao-11@sms.ed.ac.uk, yftah.ziser@ed.ac.uk, scohen@inf.ed.ac.uk

Abstract

We describe a simple and effective method (Spectral Attribute removalL; SAL) to remove guarded information from neural representations. Our method uses singular value decomposition and eigenvalue decomposition to project the input representations into directions with *reduced* covariance with the guarded information rather than *maximal* covariance as normally these factorization methods are used. We begin with linear information removal and proceed to generalize our algorithm to the case of nonlinear information removal using kernels. Our experiments demonstrate that our algorithm retains better main task performance after removing the guarded information compared to previous methods. In addition, our experiments demonstrate that we need a relatively small amount of guarded attribute data to remove information about these attributes, which lowers the exposure to such possibly sensitive data and fits better low-resource scenarios.¹

1 Introduction

Natural language processing (NLP) models currently play a critical role in decision-supporting systems. These models' predictions are often affected by undesirable biases encoded in the real-world data they are trained on. Making sensitive predictions while considering irrelevant input attributes such as gender, race, religion, or demographic (**protected** or **guarded** attributes) impacts user trust and the practical broad applicability of NLP methods.

In recent years, representation learning approaches have become the mainstay of input encoding in NLP. While representation learning has yielded state-of-the-art results in many NLP tasks, it is hard to control or inspect the information encoded in these representations. Thus, using rule-based methods to remove unwanted information

from such representations is often not feasible. In the context of protected attributes, Bolukbasi et al. (2016) showed that word embeddings trained on the Google News corpus encode gender stereotypes. Later, Manzini et al. (2019) expanded this work and showed that word embeddings trained on the Reddit L2 corpus (Rabinovich et al., 2018) encode race and religion biases.

We propose a simple yet effective technique to remove information about protected attributes from neural representations. Our method, dubbed **SAL** for Spectral Attribute removalL,² applies Singular Value Decomposition (SVD) on a covariance matrix between the input representation and the protected attributes and prunes away highly co-varying directions.

In addition, we overcome the **linear removal limitations** of SAL and previous work by using eigenvalue decomposition of **kernel matrices** to obtain projections into directions with reduced covariance in the kernel feature space. We refer to this method as **kSAL** (for kernel SAL). Nonlinear removal of information from neural representations has been an open problem.

SAL outperforms the recent method of Ravfogel et al. (2020) aimed at solving the same problem, mainly in the aspect of being able to remove guarded information while retaining better performance of the main task. Further experiments demonstrate that our method performs well even when the available data for the protected attributes is limited.

2 Problem Formulation and Notation

For an integer n we denote by $[n]$ the set $\{1, \dots, n\}$. For a vector \mathbf{v} , we denote by $\|\mathbf{v}\|_2$ its ℓ_2 norm. Matrices and vectors are in boldface font (with uppercase or lowercase letters, respectively). Random variable vectors are also denoted

¹Please contact the authors for code and data.

²Also after the main character of the 2018 movie “Anon.”

by boldface uppercase letters. For a matrix \mathbf{A} , we denote by \mathbf{A}_j its j th column (or by $\mathbf{A}_{i:j}$ the matrix with columns \mathbf{A}_k for $k = i, \dots, j$). Vectors are assumed to be column vectors.

In our problem formulation, we assume the existence of three random variables: $\mathbf{X} \in \mathbb{R}^d$, $\mathbf{Y} \in \mathbb{R}$ and $\mathbf{Z} \in \mathbb{R}^{d'}$. Samples of \mathbf{X} are the inputs for a classifier to predict corresponding samples of \mathbf{Y} . The random vector \mathbf{Z} represents the guarded attributes. We would like to maximize the ability to predict \mathbf{Y} from \mathbf{X} , while minimizing the ability to predict \mathbf{Z} from \mathbf{X} . Without loss of generality, we assume that the mean values of \mathbf{X} , \mathbf{Y} and \mathbf{Z} are 0, and that $d' \leq d$.³

We assume n samples of $(\mathbf{X}, \mathbf{Y}, \mathbf{Z})$, denoted by $(\mathbf{x}^{(i)}, \mathbf{y}^{(i)}, \mathbf{z}^{(i)})$ for $i \in [n]$. These samples are used to train the classifier to predict the target values (ys) from the inputs (xs). These samples are also used to remove the information from the inputs based on the guarded attributes (zs).

3 Using Principal Directions to Erase Information

We describe SAL in this section. We explain the use of SVD on cross-covariance matrices (§3.1) and describe the core algorithm in §3.2.

3.1 SVD on Cross-covariance Matrix

Let $\mathbf{A} = \mathbb{E}[\mathbf{X}\mathbf{Z}^\top]$, the matrix of cross-covariance between \mathbf{X} and \mathbf{Z} . In that case, $\mathbf{A}_{ij} = \text{Cov}(\mathbf{X}_i, \mathbf{Z}_j)$ for $i \in [d]$ and $j \in [d']$.

A simple observation is that for any two vectors $\mathbf{a} \in \mathbb{R}^d$, $\mathbf{b} \in \mathbb{R}^{d'}$, the following holds due to the linearity of expectation:

$$\mathbf{a}\mathbf{Ab}^\top = \text{Cov}(\mathbf{a}^\top \mathbf{X}, \mathbf{b}^\top \mathbf{Z}). \quad (1)$$

This motivates the use of the cross-covariance matrix to find the so-called principal directions: directions in which the projection of \mathbf{X} and \mathbf{Z} maximize their covariance, where the projections are represented as two matrices $\mathbf{U} \in \mathbb{R}^{d \times d'}$ and $\mathbf{V} \in \mathbb{R}^{d' \times d'}$. Each column in these matrices plays the role of the vectors \mathbf{a} and \mathbf{b} in Eq. 1. More specifically, we find \mathbf{U} and \mathbf{V} such that for any

³For example, \mathbf{Z} may be a multi-class label such as gender represented as a short vector over $\{-1, 1\}$ and \mathbf{X} may be a complex input, which before removal of information about the guarded attribute \mathbf{Z} , can be used to predict \mathbf{Z} . Example of \mathbf{X} would be an encoding of a post on a message board.

$i \in [d']$ it holds that:

$$\text{Cov}(\mathbf{U}_i^\top \mathbf{X}, \mathbf{V}_i^\top \mathbf{Z}) = \max_{(\mathbf{a}, \mathbf{b}) \in \mathcal{O}_i} \text{Cov}(\mathbf{a}^\top \mathbf{X}, \mathbf{b}^\top \mathbf{Z}),$$

where \mathcal{O}_i is the set of pairs of vectors (\mathbf{a}, \mathbf{b}) such that $\|\mathbf{a}\|_2 = \|\mathbf{b}\|_2 = 1$, \mathbf{a} is orthogonal to $\mathbf{U}_1, \dots, \mathbf{U}_{i-1}$ and similarly, \mathbf{b} is orthogonal to $\mathbf{V}_1, \dots, \mathbf{V}_{i-1}$.

It can be shown that such maximization can be done by applying the SVD on \mathbf{A} such that $\mathbf{A} = \mathbf{U}\Sigma\mathbf{V}^\top$, where $\mathbf{U} \in \mathbb{R}^{d \times d}$, $\Sigma \in \mathbb{R}^{d \times d'}$ and $\mathbf{V} \in \mathbb{R}^{d' \times d'}$. In the case of SVD, \mathbf{U} and \mathbf{V} are orthonormal matrices, and Σ is a diagonal matrix with non-negative values on the diagonal. We let the vector of singular values on the diagonal of Σ be denoted by $\sigma_1, \dots, \sigma_{d'}$.

Once the orthogonal matrices in the form of \mathbf{U} and \mathbf{V} are found, one can truncate them (for example, use only a subset of the columns of \mathbf{U} , represented as the semi-orthonormal matrix $\hat{\mathbf{U}}$) to use, for example, $\hat{\mathbf{U}}^\top \mathbf{X}$, as a representation (linear projection) of \mathbf{X} which co-varies the most with \mathbf{Z} .

We suggest that rather than using the largest singular value vectors in \mathbf{U} to project \mathbf{X} , we should project \mathbf{X} using the principal directions with the **smallest** singular values. This means we find a representative of \mathbf{X} that co-varies the *least* with \mathbf{Z} , essentially removing the information from \mathbf{X} that is most related to \mathbf{Z} and can be detected through covariance.

In addition, once such a projection matrix $\bar{\mathbf{U}}$ is calculated, we can use the projection $\bar{\mathbf{X}} = \bar{\mathbf{U}}\bar{\mathbf{U}}^\top \mathbf{X}$ such that the value of $\mathbb{E}[\|\mathbf{X} - \bar{\mathbf{X}}\|_2]$ is minimized, while removing the information from \mathbf{X} . This allows us to potentially use the new projected values of the input random variable \mathbf{X} *without* changing a classifier that was originally trained on samples from \mathbf{X} , though as we see in §5, using the projected input as-is without retraining the classifier may lead to performance issues with our method and other methods as well.

See Appendix A for connections to Canonical Correlation Analysis and Principal Component Analysis. In all three cases of CCA, PCA and LSA (Latent Semantic Analysis; Dumais 2004), SVD or eigenvalue decomposition is used with the aim of *maximizing* the correlation or covariance between one or two random vectors. In our case, the SVD is used to minimize the covariance between projections of \mathbf{X} and \mathbf{Z} .

3.2 The SAL Algorithm

Our algorithm (SAL) follows the following procedure. First, the empirical cross-covariance matrix, estimating $\mathbb{E}[\mathbf{X}\mathbf{Z}^\top]$ is calculated:

$$\Omega = \frac{1}{n} \sum_{i=1}^n \mathbf{x}^{(i)} (\mathbf{z}^{(i)})^\top. \quad (2)$$

SVD is then performed on Ω to obtain $(\mathbf{U}, \Sigma, \mathbf{V})$. We choose an integer value k and define $\bar{\mathbf{U}} = \mathbf{U}_{(k+1):d}$. There is no reason for k to be larger than the rank of Ω . The rank of Ω is bounded from above by d and d' , the dimensions of the vectors of \mathbf{X} and \mathbf{Z} .

Then, the vectors $\mathbf{x}^{(i)}$ are projected using either $\bar{\mathbf{U}}^\top$ or $\bar{\mathbf{U}}\bar{\mathbf{U}}^\top$. The latter projection attempts to project $\mathbf{x}^{(i)}$ to the original dimensionality and space after removing the information. More specifically, $\bar{\mathbf{U}}\bar{\mathbf{U}}^\top$ is a projection matrix to the range of Ω .

The criterion we use to choose k is based on the singular values in Σ . More specifically, we choose a threshold $\alpha \geq 1$ and choose the minimal k such that $\Sigma_{11}/\Sigma_{k+1,k+1} > \alpha$.

4 Kernel Extension to SAL

To enrich the type of information that is detected as co-varying, it is possible to use two feature functions, $\phi: \mathbb{R}^d \rightarrow \mathbb{R}^m$ and $\psi: \mathbb{R}^{d'} \rightarrow \mathbb{R}^{m'}$, and apply the procedure in §3 on $\mathbb{E}[\phi(\mathbf{X})(\psi(\mathbf{Z}))^\top]$. In that case, we can erase the information from $\phi(\mathbf{X})$ and treat it as the input for further classification. If the classifier is already learned, it would have to take input vectors of the form $\phi(\mathbf{X})$, otherwise it can be re-trained with the erased inputs.

4.1 The Kernel Trick

The kernel trick refers to learning and prediction without explicitly representing $\phi(\mathbf{x})$ or $\psi(\mathbf{z})$. Rather than that, we assume two kernel functions, $K_\phi(\mathbf{x}, \mathbf{x}')$ and $K_\psi(\mathbf{z}, \mathbf{z}')$ that calculate similarities between two \mathbf{x} s or between two \mathbf{z} s.

Every kernel that satisfies the necessary properties can be shown to be a dot product in some feature space. This means that for a given kernel function $K_\phi(\mathbf{x}, \mathbf{x}')$ it holds that

$$K_\phi(\mathbf{x}, \mathbf{x}') = \langle \phi(\mathbf{x}), \phi(\mathbf{x}') \rangle, \quad (3)$$

for some ϕ function and similarity for $K_\psi(\mathbf{z}, \mathbf{z}')$. Masking learning and prediction through a kernel function is often useful when the feature representations ϕ and ψ are hard to explicitly compute, for

example, because $m = \infty$ or $m' = \infty$ (such as the case with the Radial Basis Function, RBF, kernel).

We show next that the kernel trick can be used to generalize SAL to nonlinear information removal in §3.1.

4.2 Removal with the Kernel Trick

Rather than assuming a set of examples in the form mentioned in §2, we assume we are given as input two kernel matrices of dimension $n \times n$:

$$[\mathbf{K}_\phi]_{ij} = K_\phi(\mathbf{x}^{(i)}, \mathbf{x}^{(j)}), \\ [\mathbf{K}_\psi]_{ij} = K_\psi(\mathbf{z}^{(i)}, \mathbf{z}^{(j)}).$$

In addition, for the justification of our algorithm, we define the following two feature matrices based on the kernel feature functions:

$$\forall i \in [m], j \in [n] \quad [\Phi]_{ij} = \phi(\mathbf{x}^{(j)})_i, \\ \forall i \in [m'], j \in [n] \quad [\Psi]_{ij} = \psi(\mathbf{z}^{(j)})_i.$$

Note that these two matrices are never calculated explicitly. Given the definition of the kernel as a dot product in the feature space (Eq. 3), it can be shown that $\mathbf{K}_\phi = \Phi^\top \Phi$ and $\mathbf{K}_\psi = \Psi^\top \Psi$. In addition, we slightly change the empirical cross-covariance matrix Ω definition in Eq. 2 to: $\Omega = \Phi \Psi^\top$. (This means we ignore the constant $1/n$ in the above definition of Ω that normalizes the matrix with respect to the number of examples. This does not change the nature of the following discussion, but makes it simpler.) At this point, the question is how to perform SVD on Ω without ever accessing directly the feature functions. This is where spectral theory of matrices comes in handy.

More specifically, it is known that the left singular vectors of Ω (\mathbf{U}) are the eigenvectors of $\Omega \Omega^\top$. In addition, the singular values of Ω correspond to the square-root values of the eigenvalues of $\Omega \Omega^\top$.

In addition, we show in Appendix B why an eigenvector \mathbf{w} of $\Gamma = \mathbf{K}_\phi \mathbf{K}_\psi$ can be transformed to an eigenvector of $\Omega \Omega^\top$ by multiplying \mathbf{w} on the left by Φ and calculating $\Phi \mathbf{w}$.

With this fact in mind, we are now ready to find the left singular vectors of Ω by finding the eigenvalues of Γ , a matrix which is solely based on the kernel functions of \mathbf{x} and \mathbf{z} .

Let $\mathbf{w}_1, \dots, \mathbf{w}_k$ be eigenvectors of Γ and let $\mathbf{w}'_1, \dots, \mathbf{w}'_k$ be the orthonormalization of \mathbf{w}_i , $i \in [k]$ based on the inner product $\langle \mathbf{w}_i, \mathbf{w}_j \rangle =$

$\mathbf{w}_i \mathbf{K}_\phi \mathbf{w}_j^\top$. If we denote by \mathbf{W} the matrix such that $\mathbf{W}_j = \mathbf{w}'_j$ for $j \in [k]$, then $\Phi \mathbf{W} = \mathbf{U}$ where \mathbf{U} is the left singular vector matrix of Ω . Then,

$$\mathbf{U}^\top \phi(\mathbf{x}) = (\mathbf{W}^\top \Phi^\top) \phi(\mathbf{x}) = \mathbf{W}^\top \kappa(\mathbf{x}), \quad (4)$$

where $\kappa(\mathbf{x})$ is a function that returns a vector of length n such that $[\kappa(\mathbf{x})]_j = K(\mathbf{x}^{(j)}, \mathbf{x})$. Eq. 4 implies that we are able to calculate the projection of $\phi(\mathbf{x})$ while removing the information in $\psi(\mathbf{z})$ by using the eigenvectors of Γ with smallest eigenvalues and kernel calculations of each training example with \mathbf{x} .

4.3 Practical Kernel Removal

Using the kernel algorithm as above may lead to issues with tractability, as it possibly requires calculating the full eigenvector matrix of a large matrix (the product of two kernel matrices). We propose an alternative algorithm (kSAL) for the kernel case which is more tractable.

For a fixed $0 \leq k \leq n$ (which does not need to be larger than the rank of either kernel matrices), we compute only the top k eigenvectors of Γ . We then compute an orthonormal basis for the nullspace of the matrix $(\mathbf{K}_{\phi,1/2} \mathbf{W}_{1:k})^\top$ where

$$\mathbf{K}_{\phi,1/2} = \mathbf{U}_\phi \Sigma_\phi^{1/2} \mathbf{V}_\phi^\top,$$

with $(\mathbf{U}_\phi, \Sigma_\phi, \mathbf{V}_\phi)$ being the SVD of \mathbf{K}_ϕ . Practically, this means we find a matrix $\mathbf{L}_\phi \in \mathbb{R}^{n \times (n-d)}$ such that $\mathbf{L}_\phi^\top \mathbf{L}_\phi = I$ and that $\|(\mathbf{K}_{\phi,1/2} \Gamma)^\top \mathbf{L}_\phi\|_2 \approx 0$. The final data points $\hat{x}^{(j)}$ we use further down the pipeline correspond to the rows of $\mathbf{K}_{\phi,1/2} \mathbf{L}_\phi \in \mathbb{R}^{n \times (n-k)}$. If we are interested in using directly the reduced kernel matrix for the input vectors, we can use

$$\hat{\mathbf{K}}_\phi = \mathbf{K}_{\phi,1/2} \mathbf{L}_\phi \mathbf{L}_\phi^\top \mathbf{K}_{\phi,1/2}^\top. \quad (5)$$

Time Complexity Absorbing the kernel function computation as a constant, computing the kernel matrices is $\mathcal{O}(n^2)$ and their product Γ in $\mathcal{O}(n^\omega)$ for $\omega < 2.808$ using Strassen’s algorithm, but can be done much more efficiently when \mathbf{K}_ψ is sparse, as normally expected. Calculating the top k eigenvectors of Γ , has a cost of $\mathcal{O}(nk^2 + k^3)$ using, for example, the Arnoldi method.⁴ In §5.1, we report clock running time for the kernel method.

⁴For example, Matlab implements a variant of the Arnoldi method for its function `eigs`.

	SL999	WS353-S	WS353-R	Mturk-771
Before	0.371	0.695	0.6	0.684
After	0.391	0.7	0.605	0.698

Table 1: The semantic evaluation of word embeddings before and after removing gender bias.

Below, we experiment with a variety of kernel functions, more specifically with RBF kernels (where $K_\phi(\mathbf{x}, \mathbf{x}') = \exp(-\gamma \|\mathbf{x} - \mathbf{x}'\|_2^2)$; we use $\gamma = 0.1$) and polynomial kernel of degree 2 (where $K_\phi(\mathbf{x}, \mathbf{x}') = (1 + \mathbf{x}^\top \mathbf{x}')^2$). “Linear kernel” refers to standard dot product. The kernel of \mathbf{z} remains linear.

5 Experiments

In our experiments, our main comparison algorithm is the iterative nullspace projection (INLP) algorithm of [Ravfogel et al. \(2020\)](#) (NIO2020), which aims at solving an equivalent problem to ours. For the word embedding debiasing and fair classification (both setups), we replicate the experimental settings of [Ravfogel et al. \(2020\)](#).⁵ SAL provides linear guarding, similarly to INLP, while kSAL also captures nonlinear regularities with respect to \mathbf{Z} . We can provide such guarding for representations of state-of-the-art encoders (such as BERT), provided the representations are eventually fed into a classifier for prediction. The protected attributes we experiment with include *gender* and *race*.

5.1 Word Embedding Debiasing

Word embeddings are often prone to encode biases in various ways (see §6). We evaluate our methods on gender bias removal from GloVe word embeddings. We use the 150,000 most common words and discard the rest. We sort the embeddings by their projection on the $\overrightarrow{\text{he}}$ - $\overrightarrow{\text{she}}$ direction. Then we consider the top 7,500 word embeddings as male-associated words ($z = 1$) and the bottom 7,500 as female-associated words ($z = -1$). We follow NIO2020 train/validation/test split sizes and data (49%/21%/30%).

Results with SAL A linear classifier can perfectly predict the guarded gender attribute when trained on out-of-the-box Glove embeddings. Removing the first direction ($k = 1$) does not affect accuracy. For $k = 2$, the performance drops to

⁵We use the authors’ implementation for both the INLP method and the experimental settings: https://github.com/shauli-ravfogel/nullspace_projection.

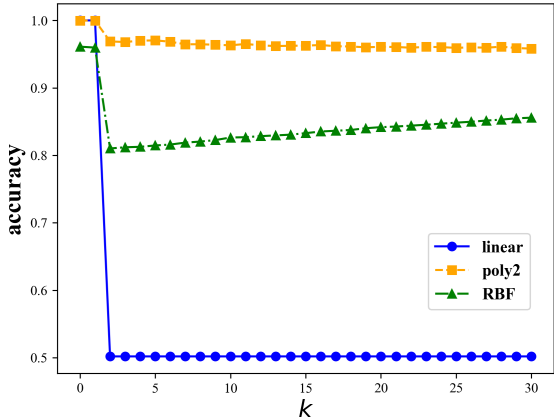


Figure 1: A classifier accuracy for gender prediction as a function of the number of principal directions that are linearly removed. For the linear classifier, we use a linear SVM. For the nonlinear classifiers, we use SVM with the polynomial kernel and with the RBF kernel.

50.2%, close to a random guess. We further perform intrinsic semantic tests to ensure the debiased embeddings remain useful. We use SimLex-999, WordSim353, and Mturk771 (similarity and relatedness datasets) to calculate the correlation between cosine similarities of the word embeddings to the human-annotated similarity score (Hill et al., 2015; Finkelstein et al., 2001; Halawi et al., 2012). We observed minor improvements for all three tests when using debiased embeddings (Table 1), suggesting that our method keeps the embeddings intact. In addition, we report the three most similar words (nearest neighbors) for ten random words before and after we apply SAL (see Appendix B). We observe almost no change between the two sets of embedding results.

SAL debiasing does not provide a nonlinear information removal. In Figure 1 we plot the performance of nonlinear classifiers in the prediction of the **linearly-guarded** attribute (gender) as a function of the number of removed directions. We also provide linear classifier results for reference. We see that even after removing up to 30 principal directions, (linear) SAL is not sufficient for nonlinear classifiers – the gender can still be predicted. This finding is also noted by Ravfogel et al. (2020), who did not offer a direct solution. This finding partially motivates our development of kSAL.

Kernel Debiasing All three kernels achieve high gender prediction accuracy when no information is removed ($k = 0$), with accuracy of 100%, 99.9% and 95.7% for the linear, polynomial, and RBF kernel, respectively. While the performance of the

linear and polynomial kernels is not affected by removing one principal direction ($k = 1$), the RBF kernel accuracy drops to 86.3%. With $k = 2$, performance drops to 50.2%, 44.5% and 50.2% for the linear, polynomial, and RBF kernel, respectively, under **nonlinear kernel** removal. Compared to Figure 1 with SAL, we see kSAL effectively removes nonlinear information.

Deviations of Reduced Kernel from Original Kernel

To quantitatively test whether the embeddings retain their geometric form when removing gender information, we compare the standard deviation (ρ) of the values in \mathbf{K}_ϕ to the average deviation (γ) of values of \mathbf{K}_ϕ from the corresponding values in $\hat{\mathbf{K}}_\phi$ (Eq. 5). When removing two principal directions, the largest approximation difference is seen in the linear kernel, with $\gamma/\rho = 0.64$. For the polynomial kernel, we observe $\gamma/\rho = 0.52$. For RBF, we have $\gamma/\rho = 0.16$.

5.2 Fair Classification

To further evaluate our method on downstream tasks, we follow the fair classification tests of Ravfogel et al. (2020).

5.2.1 Fair Sentiment Analysis

Task and Data The first task is sentiment analysis for social network users’ posts. We use the TwitterAAE dataset (Blodgett et al., 2016), which contains users’ tweets (\mathbf{x}), coupled with the users’ ethnic affiliations (\mathbf{z}), and a binary label for the sentiment the tweet conveys (\mathbf{y}). The dataset splits the users into two groups, African American English (AAE) speakers and Standard American English (SAE) speakers. As users’ privacy makes it hard to obtain ground truth labels for ethnic affiliation, the dataset uses the demographics of the neighborhoods the users live in as a proxy. Following NIO2020, we use the encoder of Felbo et al. (2017), DeepMoji, to obtain the tweets representation. DeepMoji is suitable for our goal, as it has been shown to encode demographic information, and therefore, might lead to unfair classification (Elazar and Goldberg, 2018).

We experiment with four different setups. The dataset consists of an equal amount of positive and negative sentiment examples for all of them. The datasets differ with respect to the guarded attribute ratio. For example, a ratio of 0.8 means that 0.8 of the positive sentiment class examples are composed of AAE speakers, and 0.2 is composed of

Ratio	Sentiment				TPR-Gap			
	Orig.	INLP	SAL, $k = 1$	SAL, $k = 2$	Orig.	INLP	SAL, $k = 1$	SAL, $k = 2$
0.5	0.765	0.763	0.765	0.767	0.146	0.12	0.145	0.11
0.6	0.753	0.757	0.753	0.753	0.226	0.191	0.228	0.09
0.7	0.741	0.748	0.735	0.736	0.319	0.263	0.316	0.116
0.8	0.72	0.529	0.715	0.719	0.404	0.011	0.365	0.186

Table 2: The sentiment analysis scores (we use accuracy, as the dataset is balanced) and TPR differences (lower is better) as a function of the ratio of tweets written by black individuals and conveying positive sentiment.

SAE speakers. We experiment with ratios of 0.5, 0.6, 0.7 and 0.8. The larger the ratio, the higher the classifier’s tendency to make use of protected attributes to make its prediction.

Evaluation Measures We report the accuracy of the methods on the sentiment analysis task. To measure fairness, we use the difference in true positive rate (TPR-gap) between individuals belonging to different guarded attributes groups (Hardt et al., 2016; Ravfogel et al., 2020). The rationale behind TPR-gap is that for an equal opportunity, a positive outcome must be independent of the guarded attribute (z), conditional on (y) being an actual positive. See Hardt et al. (2016) for more details.

Results Table 2 presents our results for the fair sentiment classification. For the first three ratios, 0.5, 0.6, and 0.7, we can see that both SAL ($k = 1, 2$) and INLP (Ravfogel et al., 2020) maintain most of the main-task performance. In debiasing (TPR-Gap), SAL with $k = 2$ significantly outperforms INLP. As expected, removing two directions results in better debiasing than removing one, but it does not lead to a performance drop on the main task. While for the last ratio, 0.8, INLP achieves the highest TPR-gap result, it comes at the cost of a sharp performance drop on the main task, resulting in a nearly random classifier. SAL ($k = 1, 2$) maintains most of the main-task performance, and for $k = 2$, the TPR-gap is halved.

5.2.2 Fair Profession Classification

Task and Data The second task is profession classification. De-Arteaga et al. (2019) attempt to quantify the bias in automatic hiring systems, as they are critical and can drastically affect people’s lives. They show that even for a simple task, predicting candidate profession based on self-provided short biography, significant gaps result from the writer gender. This might influence the open positions an automatic system will recommend to a candidate, thus favoring candidates from one gen-

der over the other. We hence follow the setup of De-Arteaga et al. (2019), who experiment with professions classification (y), from short biographies (x), and gender as a guarded attribute (z). We follow the dataset splits of Ravfogel et al. (2020), resulting in approximately 75K training examples (65%), 12K development examples (10%), and 29K (25%) test examples. We use a multiclass classifier to predict the profession, as there are 28 profession classes. We experiment with two types of text representations, FastText (Joulin et al., 2016), based on bag of word embeddings (BWE) and BERT (Devlin et al., 2018) encodings.

Evaluation Measures We report accuracy for the profession classification. For bias level measurement, we use a generalization of TPR-gap for multi-class, suggested by De-Arteaga et al. (2019), calculating the root mean square (RMS) of the TPR with respect to all classes.

De-Arteaga et al. (2019) also provided evidence for a strong correlation between TPR-gap and existing gender imbalances in occupations, which may lead to unfair classification.

Results Table 3 presents the profession classification results. Similar to the sentiment analysis task, SAL ($k = 1, 2$) maintains most of the main-task performance, and for $k = 2$, the two-direction removal, the TPR-gap is lower. When comparing SAL ($k = 2$) to INLP, we observe a clear trade-off between maintaining the main task performance (SAL, $k = 2$) and low TPR-gap scores (INLP).

5.3 Scarce Protected Attribute Labels

For many real-world applications, obtaining large amounts of labeled data for protected attributes can be costly, labor-intensive, and in some cases, infeasible due to an ever-increasing number of privacy regulations. In this analysis, we stress-test our algorithm by simulating a scenario in which only a limited amount of samples from the downstream

Encoder	Accuracy (profession)				TPR-Gap (RMS)			
	Orig.	INLP	SAL, $k = 1$	SAL, $k = 2$	Orig.	INLP	SAL, $k = 1$	SAL, $k = 2$
FastText	0.755	0.715	0.76	0.76	0.201	0.09	0.186	0.12
BERT	0.8	0.693	0.786	0.786	0.214	0.065	0.178	0.096

Table 3: The profession classification on the biographies dataset results. We report accuracy and TPR-RMS. The number of classes is 28.

task are coupled with the desired protected attribute labels. For this purpose, we replicate the fair sentiment classification experiments, but this time, feeding only a fraction of the annotated data to our debiasing method. In terms of the main task, the experiment is identical, i.e., we use 100K samples for training the sentiment classifier. We experiment with different fractions of the debiasing data, i.e., 5% of the sentiment training data contains labels about the protected attribute. We hence feed 5,000 samples for debiasing. The subsets for debiasing are chosen randomly. We repeat each experiment 10 times with different subsets.⁶ Table 4 presents our results. We observe that using only a small fraction of the data for debiasing did not affect SAL’s ($k = 1, 2$) ability to maintain much of the main-task performance. INLP, on the other hand, suffers from a sharp performance decrease, resulting in a near-random sentiment classifier. SAL’s ($k = 1, 2$) ability to debias the data is slightly worse than in the complete dataset setting but the resulting representations are still significantly less biased than the original ones. INLP achieves low TPR gaps, but it is hard to determine if this results from an accurate bias removal or merely a result of corrupting the representations.

5.4 Kernel Experiments

Despite their flexibility in modeling rich feature functions, kernels have been documented to be computationally intensive. Lack of computational resources prevented us from using the full sentiment and bios datasets for our kernel experiments, and instead, we use 15,000 training examples and 7,998 test set examples (the full test set) for the sentiment dataset and 15,000 training examples and 5,000 examples for the profession dataset. For training on the acquired 15,000 training examples, we used one Intel Xeon E5-2407 CPU, running at 2.2 GHz, for approximately five hours (for a time complexity analysis, see section 4.3).

⁶For brevity, we report the results for a subset of 5%. We get similar results for 0.5% and 10% subset sizes as well.

Table 5 presents our results. While using only a small subset of the data for both tasks, we can see kSAL-poly2 reduces the TPR gaps of both tasks while maintaining most of their performance on the main task. For the sentiment analysis task, kSAL-RBF slightly improves the main task results while reducing the TPR-gap (RMS). For the profession classification task With RBF, the results are unexpected, with main task performance increasing as we remove principal directions, perhaps due to the pruning of the rich, infinite feature space RBF kernel represents (we also observe significant overfitting with RBF).⁷

5.5 Perturbed Inputs

While the transformation through $\bar{U}\bar{U}^\top$ maps \mathbf{x} back into the original vector space (as a projection), it often turns out that it removes information such a way that the *original* classifier (trained on data without removal) can no longer be used with the inputs after removal. This issue exists not only with our algorithm, but also with INLP, and indeed, like us, [Ravfogel et al. \(2020\)](#) re-trained their classifier after they created the cleaned projected inputs.

Ideally, we would want to remove information without necessarily having to retrain a classifier for the main task. This is similar to a user using a service without providing details they would like to keep private. To test the effect of such an approach, we interpolated $\bar{U}\bar{U}^\top$ with the identity matrix, to eventually project \mathbf{x} using $\lambda\bar{U}\bar{U}^\top + (1 - \lambda)\mathbf{I}$ for $\lambda \in \{0, 0.1, \dots, 1.0\}$. This approach weakens the impact of the removal projection and retains some of the information in \mathbf{x} . While an adversary can attack this approach, it can mitigate the effects of privacy violations in cases where the service cannot be retrained, especially if the service has no adversarial intent.

Figure 2 describes an ablation experiment, ranging λ as above on the bios dataset. We see that as we increase the intensity of the use of the SAL pro-

⁷NIO2020 observed RBF-kernel SVM obtained low accuracy results as well

Ratio	Sentiment				TPR-Gap			
	Orig.	INLP	SAL, $k = 1$	SAL, $k = 2$	Orig.	INLP	SAL, $k = 1$	SAL, $k = 2$
0.5	0.76	0.573	0.76	0.76	0.141	0.021	0.413	0.11
0.6	0.755	0.594	0.755	0.75	0.229	0.034	0.231	0.091
0.7	0.741	0.57	0.734	0.729	0.317	0.056	0.311	0.127
0.8	0.72	0.571	0.715	0.711	0.406	0.083	0.343	0.175

Table 4: The sentiment analysis experiments, 100K samples are used to train the sentiment classifier, but only 5K examples are used for learning to remove bias. The test set is identical to the one used in section 5

Sentiment Analysis (DeepMoji)							
k	Main		TPR-Gap		poly2	rbf	poly2
	poly2	rbf	poly2	rbf			
0	0.751	0.763	0.145	0.152			
1	0.751	0.764	0.145	0.151			
2	0.75	0.765	0.13	0.12			
Profession Classification (BERT)							
k	Main		TPR-Gap (RMS)		poly2	rbf	poly2
	poly2	rbf	poly2	rbf			
0	0.773	0.616	0.335	0.239			
1	0.771	0.682	0.285	0.345			
2	0.771	0.684	0.251	0.311			

Table 5: Kernel results with kSAL for sentiment (for a ratio of 0.5) and profession classification.

jection (increasing λ), the accuracy of both gender prediction and profession prediction decrease when training the original classifier on the non-projected inputs. While the behavior is similar for the gender accuracy for both INLP and our method, the decrease is much sharper for $\lambda > 0.4$ for INLP.

6 Related Work

In their influential work, [Bolukbasi et al. \(2016\)](#) revealed that the word embeddings for many gender-neutral terms show a clear gender bias. They did so by projecting word embeddings on a clear gender direction, such as $\overrightarrow{\text{he}}$ - $\overrightarrow{\text{she}}$. To mitigate this bias, they minimized the gender-neutral embeddings projection onto pre-determined gender directions, such as the one mentioned above. [Zhao et al. \(2018\)](#) presented a customized training scheme for word embeddings, which minimizes the negative distances between words in the two groups, e.g., male and female related words, for gender debiasing. By analyzing both methods above, [Gonen and Goldberg \(2019\)](#) demonstrated that bias is deeply intertwined in word embeddings using multiple tests. For example, they showed that an RBF-kernel SVM classifier accurately predicts the gender associated with

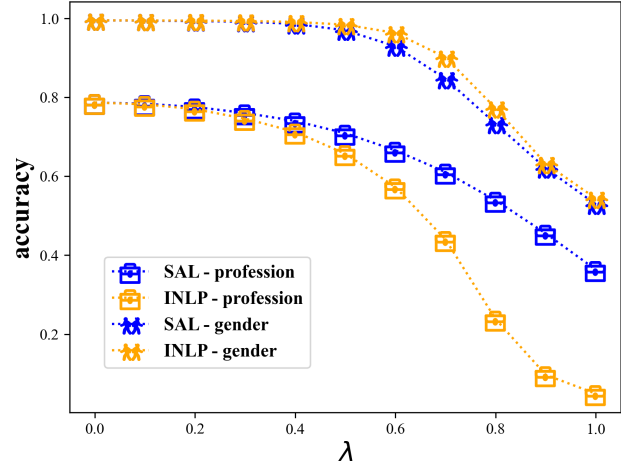


Figure 2: Gender and profession classifications as a function of the interpolation coefficient λ .

gender-neutral words, even after applying the methods mentioned above. Similar to [Ethayarajh et al. \(2019\)](#), they conclude that removing a small number of intuitively selected gender directions can not guarantee the elimination of bias. Motivated by this conclusion, [Ravfogel et al. \(2020\)](#) presented iterative nullspace projection (INLP). This debasing algorithm iteratively projects features into a space where a linear classifier can not predict the guarded attribute. The debiased representations are *linearly guarded*, i.e., they can not guarantee bias removal beyond the linear level. Indeed, they show a simple nonlinear classifier can achieve high accuracy when predicting the guarded attribute. Their approach is also related to that of [Xu et al. \(2017\)](#). Our approach stands in stark contrast to adversarial removal of information ([Edwards and Storkey, 2015; Li et al., 2018; Coavoux et al., 2018; Elazar and Goldberg, 2018; Barrett et al., 2019](#)), where information is removed by an objective function that balances the level of removal of information and the main task objective.

7 Conclusions

We presented SAL, a method for removing bias from learned representations and providing linear erasure of protected information while not affecting their usefulness. We extended our method by using kernels (kSAL), showing we can provide an effective nonlinear guarding. In addition, we demonstrated the robustness of (k)SAL to real-world low-resource situations, in which only a small guarded attribute dataset is provided for information removal.

References

Maria Barrett, Yova Kementchedjhieva, Yanai Elazar, Desmond Elliott, and Anders Søgaard. 2019. Adversarial removal of demographic attributes revisited. In *Proceedings of the 2019 Conference on Empirical Methods in Natural Language Processing and the 9th International Joint Conference on Natural Language Processing (EMNLP-IJCNLP)*, pages 6330–6335.

Su Lin Blodgett, Lisa Green, and Brendan O’Connor. 2016. Demographic dialectal variation in social media: A case study of african-american english. *arXiv preprint arXiv:1608.08868*.

Tolga Bolukbasi, Kai-Wei Chang, James Y Zou, Venkatesh Saligrama, and Adam T Kalai. 2016. Man is to computer programmer as woman is to homemaker? debiasing word embeddings. *Advances in neural information processing systems*, 29:4349–4357.

Maximin Coavoux, Shashi Narayan, and Shay B Cohen. 2018. Privacy-preserving neural representations of text. In *Proceedings of the 2018 Conference on Empirical Methods in Natural Language Processing*, pages 1–10.

Maria De-Arteaga, Alexey Romanov, Hanna Wallach, Jennifer Chayes, Christian Borgs, Alexandra Chouldechova, Sahin Geyik, Krishnaram Kenthapadi, and Adam Tauman Kalai. 2019. Bias in bios: A case study of semantic representation bias in a high-stakes setting. In *proceedings of the Conference on Fairness, Accountability, and Transparency*, pages 120–128.

Jacob Devlin, Ming-Wei Chang, Kenton Lee, and Kristina Toutanova. 2018. Bert: Pre-training of deep bidirectional transformers for language understanding. *arXiv preprint arXiv:1810.04805*.

Susan T Dumais. 2004. Latent semantic analysis. *Annual review of information science and technology*, 38(1):188–230.

Harrison Edwards and Amos Storkey. 2015. Censoring representations with an adversary. *arXiv preprint arXiv:1511.05897*.

Yanai Elazar and Yoav Goldberg. 2018. Adversarial removal of demographic attributes from text data. *arXiv preprint arXiv:1808.06640*.

Kawin Ethayarajh, David Duvenaud, and Graeme Hirst. 2019. Understanding undesirable word embedding associations. *arXiv preprint arXiv:1908.06361*.

Bjarke Felbo, Alan Mislove, Anders Søgaard, Iyad Rahwan, and Sune Lehmann. 2017. Using millions of emoji occurrences to learn any-domain representations for detecting sentiment, emotion and sarcasm. *arXiv preprint arXiv:1708.00524*.

Lev Finkelstein, Evgeniy Gabrilovich, Yossi Matias, Ehud Rivlin, Zach Solan, Gadi Wolfman, and Eytan Ruppin. 2001. Placing search in context: The concept revisited. In *Proceedings of the 10th international conference on World Wide Web*, pages 406–414.

Hila Gonen and Yoav Goldberg. 2019. Lipstick on a pig: Debiasing methods cover up systematic gender biases in word embeddings but do not remove them. *arXiv preprint arXiv:1903.03862*.

Guy Halawi, Gideon Dror, Evgeniy Gabrilovich, and Yehuda Koren. 2012. Large-scale learning of word relatedness with constraints. In *Proceedings of the 18th ACM SIGKDD international conference on Knowledge discovery and data mining*, pages 1406–1414.

Moritz Hardt, Eric Price, and Nati Srebro. 2016. Equality of opportunity in supervised learning. *Advances in neural information processing systems*, 29:3315–3323.

Felix Hill, Roi Reichart, and Anna Korhonen. 2015. Simlex-999: Evaluating semantic models with (genuine) similarity estimation. *Computational Linguistics*, 41(4):665–695.

Armand Joulin, Edouard Grave, Piotr Bojanowski, Matthijs Douze, Hervé Jégou, and Tomas Mikolov. 2016. Fasttext. zip: Compressing text classification models. *arXiv preprint arXiv:1612.03651*.

Yitong Li, Timothy Baldwin, and Trevor Cohn. 2018. Towards robust and privacy-preserving text representations. In *Proceedings of the 56th Annual Meeting of the Association for Computational Linguistics (Volume 2: Short Papers)*, pages 25–30.

Thomas Manzini, Yao Chong Lim, Yulia Tsvetkov, and Alan W Black. 2019. Black is to criminal as caucasian is to police: Detecting and removing multiclass bias in word embeddings. *arXiv preprint arXiv:1904.04047*.

Ella Rabinovich, Yulia Tsvetkov, and Shuly Wintner. 2018. Native language cognate effects on second language lexical choice. *Transactions of the Association for Computational Linguistics*, 6:329–342.

Shauli Ravfogel, Yanai Elazar, Hila Gonen, Michael Twiton, and Yoav Goldberg. 2020. Null it out: Guarding protected attributes by iterative nullspace projection. *arXiv preprint arXiv:2004.07667*.

Ke Xu, Tongyi Cao, Swair Shah, Crystal Maung, and Haim Schweitzer. 2017. Cleaning the null space: A privacy mechanism for predictors. In *Proceedings of the AAAI Conference on Artificial Intelligence*, volume 31.

Jiayu Zhao, Yichao Zhou, Zeyu Li, Wei Wang, and Kai-Wei Chang. 2018. Learning gender-neutral word embeddings. *arXiv preprint arXiv:1809.01496*.

A Connection to CCA and PCA

How is SAL related to Canonical Correlation Analysis? The use of SVD on the cross-covariance matrix is very much related to the technique of Canonical Correlation Analysis (CCA), in which projections of \mathbf{X} and \mathbf{Z} are found such that they maximize the cross-correlation between these two random vectors. Rather than applying SVD on the cross-correlation matrix (CCA), we apply it on the cross-covariance matrix to preserve the scale of \mathbf{X} in our projection.

How is SAL related to Principal Component Analysis? The use of SVD on the cross-covariance matrix is reminiscent of Principal Component Analysis (PCA), in which eigenvalue decomposition is applied on $\mathbb{E}[\mathbf{X}\mathbf{X}^\top]$ to reduce the dimensionality of \mathbf{X} . However, PCA does not reduce the dimensionality of \mathbf{X} while removing information present in the guarded r.v. \mathbf{Z} . Rather, it finds projection of \mathbf{X} in which the covariance of linear combination of \mathbf{X} with itself is maximized.

B Eigenvectors of Λ

We turn to the following Lemma used in §4.2.

Lemma 1. *Let \mathbf{w} be an eigenvector associated with eigenvalue $\lambda \in \mathbb{R}$ for $\Gamma = \mathbf{K}_\phi \mathbf{K}_\psi$. Then $\Phi\mathbf{w}$ is an eigenvector of $\Omega\Omega^\top$.*

Proof. Since \mathbf{w} is an eigenvector of Γ , it holds that $\Gamma\mathbf{w} = \lambda\mathbf{w}$. Therefore:

$$\begin{aligned} \Psi^\top \Psi \Phi^\top \Phi \mathbf{w} &= \lambda \mathbf{w}, \\ (\Phi \Psi^\top \Psi \Phi^\top) \Phi \mathbf{w} &= \lambda \Phi \mathbf{w}, \end{aligned}$$

and therefore $\Phi\mathbf{w}$ is an eigenvalue of

$$\Omega\Omega^\top = \Phi \Psi^\top \Psi \Phi^\top.$$

□

C Nearest Neighbors Test for Word Embedding Debiasing

We give in Table 6 the ten nearest neighbor words for ten random words from the data, before and after using SAL. The neighboring words are determined through cosine similarity of the corresponding embeddings with respect to the pivot word embedding. We observe little to no difference in these two lists (before and after).

Words	Nearest neighbours before	Nearest neighbours after
lobbying	lobbyists, lobbyist, campaigning	lobbyists, lobbyist, campaigning
once	again, then, when	again, then, when
parliament	parliamentary, mps, elections	parliamentary, mps, elections
dashboard	dashboards, smf, powered	dashboards, smf, powered
cumulative	gpa, accumulative, aggregate	gpa, accumulative, aggregate
foam	rubber, mattress, polyurethane	rubber, mattress, polyurethane
rh	lh, bl, r	lh, bl, graphite
genetically	gmo, gmos, genetic	gmo, gmos, genetic
inner	outer, inside, innermost	outer, inside, innermost
harvest	harvesting, harvests, harvested	harvesting, harvests, harvested

Table 6: Nearest neighbor test on GloVe word embeddings before and after debiasing on gender